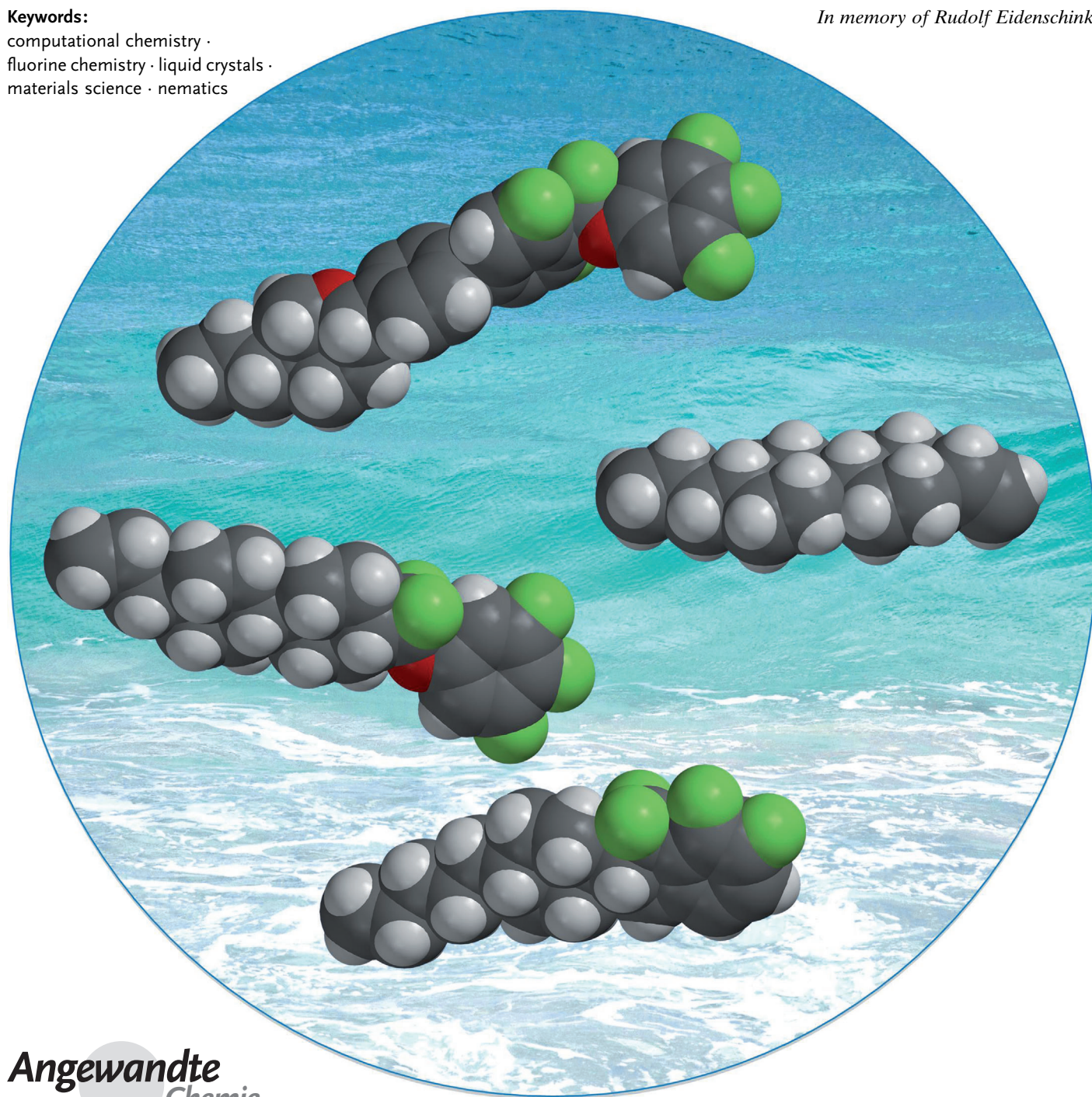# The TV in Your Pocket: Development of Liquid-Crystal Materials for the New Millennium

Matthias Bremer,* Peer Kirsch,* Melanie Klasen-Memmer, and Kazuaki Tarumi

In memory of Rudolf Eidenschink

8880   www.angewandte.org

© 2013 Wiley-VCH Verlag GmbH & Co. KGaA, Weinheim

Angew. Chem. Int. Ed. **2013,** *52,* 8880 – 8896

Angewandte *Chemie*

New liquid crystals with very low viscosity, good mesophase behavior, and high reliability are necessary to achieve the breakthrough from flat computer monitors to large displays for television. Fluorine plays a decisive role not only because of the polarity it induces in organic molecules but also because of its low polarizability and weak propensity for ion solvation. In addition, subtle stereoelectronic effects in fluorine-containing liquid crystals influence material properties and allow these to be tuned to some extent to achieve the desired outcome. Some fairly sophisticated chemistry is required that is normally ruled out in the specialty chemicals industry because of cost. The television display market is now entering a phase of saturation. The broad availability of the internet has led to an ever increasing tendency for mobile products. Tablet PCs and smartphones require touch-panel functionality and low power consumption. New LCD modes with high-performance liquid crystals and additional components, such as polymerizable materials, can be used in such products.

From the Contents

1. Introduction

Over the last decade every aspect of our daily lives has become saturated with electronic devices, most of them with a display as the user interface. The vast majority of these displays in flat-screen TV sets, PC monitors, notebooks, tablet PCs, as well as in smartphones are based on liquid-crystal display (LCD) technology. With the advent of high-resolution, full-color displays using active matrix driving (AM-LCDs) in the late 1980s, the material requirements for liquid crystals changed dramatically. While for many years simple twisted nematic (TN)[1] and super-twisted nematic (STN)[2] displays used materials containing cyano and ester groups to generate the necessary polarity, these appeared to be unsuitable for AM applications because of the so-called reliability problems of such compounds.[3] It was assumed that impurities in the liquid crystal were responsible, and accordingly much effort was expended to purify the various organic compounds comprising the liquid-crystal mixture and the mixture itself. However, the problems could not be solved that way. Only new materials, which did not contain cyano and ester groups but contained fluorinated functional groups instead, were able to fulfill the new "reliability" requirements. As a result of the high resolution and the active matrix driving scheme, the voltage-holding behavior of the individual picture elements was now much more stringent. A voltage drop during the picture refresh cycle results immediately in visible lower contrast and thus poor picture quality. Therefore, the 1990s were dominated by the introduction of new fluorinated liquid crystals,[4] which aimed at both a better voltage holding behavior as well as lower viscosities to achieve faster switching times for moving pictures. In a matter of only a few years, this development led to the complete replacement of clumsy cathode ray tube (CRT) computer monitors with sleek LC displays in offices and homes throughout the world.

The next target was television. To build a large flat-screen television set, it is not sufficient to simply increase the size of a computer monitor and leave everything else constant. Televisions need much higher contrast, better viewing angle dependence of the contrast, and—a new and characteristic requirement for TV—the ability to show moving pictures without blurring effects. In the early 2000s, the goal was finally achieved with liquid crystals of even lower viscosity, excellent voltage holding properties, and stability at both low and high temperatures. Modified LC modes such as vertical alignment (VA) provided the intrinsically better contrast and excellent viewing angles.

At the beginning of the second decade of the new millennium, we have now witnessed a saturation of the LCD-TV market. These days, TVs are really big, really thin, provide very good contrast and wide viewing angles, and have become very affordable. What will be the next display product consumers will really want to buy? For a number of years 3D TVs with or without glasses have been available, but have not really caught on yet. At the time of writing this Review, more and more ultrahigh-resolution TVs are available to the consumer, but there is no commercial content available to speak of—neither by TV providers nor on storage media similar to DVDs or Blu-Ray. Even simple stylistic elements such as narrow bezels for TVs can also have an impact on the requirements for new LC materials.

[*] Dr. M. Bremer, Prof. Dr. P. Kirsch, Dr. M. Klasen-Memmer,
Dr. K. Tarumi
Merck KGaA, Liquid Crystal R&D
Frankfurter Strasse 250, 64293 Darmstadt (Germany)
E-mail: matthias.bremer@merckgroup.com
        peer.kirsch@merckgroup.com

Finally, large displays based on organic light-emitting diode (OLED) instead of LCD technology have been developed repeatedly as prototypes and have been announced as commercial products. All commercial products are currently delayed, and will undoubtedly bear hefty price tags if they finally do make it to the market.

Liquid crystals are uniquely characterized by their anisotropy of physical properties, such as the refractive index or the dielectric constant, while being fluids of relatively low viscosity. Today, all LCDs use the nematic phase, where LC molecules have a long-range orientational order compared with molecular dimensions. The liquid crystal is inserted between two glass plates, where alignment layers on both interior surfaces of the LC cell define the orientation order of the LC molecules. A light source behind the cell together with a polarizer generates linearly polarized light that enters the cell. Voltages can be applied through transparent electrodes, and, caused by the dielectric properties of the liquid crystal, the optical characteristics can be changed so that transmission through a polarizer at the other side of the cell can be controlled. The cell thickness itself needs to be adjusted according to the optical anisotropy (Δn) of the LC material, and colors are created by RGB color filters in front of each subpixel. In other words, the passage of white light through color filters can be electronically modified, thereby generating a picture that is made up of a matrix of many individual small elements, the so-called pixels.

2. Liquid-Crystal Materials for AMD Applications

The polar liquid crystals used for passive matrix (PM) display applications, such as **1** or **2**, exhibit positive dielectric anisotropy ($\Delta\varepsilon = \varepsilon_{\parallel} - \varepsilon_{\perp}$), that is, the molecular dipole vector is oriented with the long molecular axis, and the parallel dielectric constant is larger than the perpendicular one (Scheme 1).
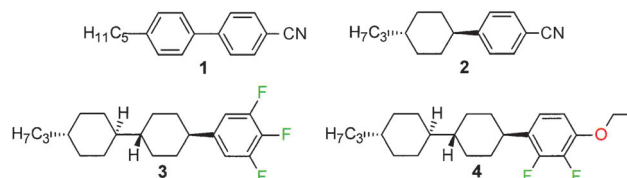
Scheme 1. Examples of liquid crystals commonly used in LCDs.

This was also true for the first fluorinated LCs used in active matrix displays. The molecular dipole moment of **3** is oriented with the long molecular axis, and, in an electric field, the rodlike molecules will align parallel to the field. The opposite behavior is found for materials such as **4**, where the dipole moment is perpendicular to the long axis. Here, the perpendicular dielectric constant is larger than the parallel one and the dielectric anisotropy is negative.[5]

The first broadly employed LCD technology was the twisted nematic (TN) mode involving materials with positive dielectric anisotropy. The orientation of LC molecules is

Matthias Bremer studied chemistry at the University of Erlangen-Nuremberg and earned a PhD in 1989 with Paul von Ragué Schleyer. After postdoctoral research at the University of California at Berkeley with Andrew Streitwieser he joined Merck KGaA in Darmstadt. Currently, he heads a research group synthesizing liquid crystals for device applications. He has served on the Editorial Boards of "Advanced Functional Materials" and "New Journal of Chemistry", and is a board member of the German Liquid Crystal Society. Since 2009 he has taught a course on "Functional Organic and Soft Materials" at the Justus-Liebig-University Giessen.

Melanie Klasen-Memmer studied Chemistry at the Technical University Kaiserslautern, Germany, where she also obtained her PhD with Hans-Georg Kuball in 1996. In 1998 she joined Merck KGaA in Darmstadt, Germany and is currently heading a group in the Physical Liquid Crystals research department. She has published several research papers and patents on liquid crystal materials for display applications.

Peer Kirsch received his PhD from the University of Heidelberg with Heinz A. Staab. After postdoctoral research at the Institute of Physical and Chemical Research (RIKEN) in Saitama, Japan, with Tomoya Ogawa he joined the Liquid Crystal Division of Merck KGaA, in 1995, and held various positions in R&D and business development in both Germany and Japan. He completed his habilitation in 2001 at the University of Bremen, and is visiting professor at the University of Freiburg. His scientific interests—besides liquid crystals—lie in the areas of fluorine chemistry and organic and molecular electronics.

Kazuaki Tarumi studied physics at Waseda University in Japan and received an MSc in 1976. After a scholarship (DAAD) he worked as a research assistant at the University of Bremen, Germany (1981—1987), where he received a PhD in theoretical physics in 1985 with Helmut Schwegler. From 1987 to 1990, he was an assistant professor in the Department of Physics at Gunma University in Japan. He joined Merck KGaA in Germany in 1991 and works in the Physical Liquid Crystal Research department. Since 1998 he has been Senior Director of the physics department.

twisted 90° through the liquid crystalline bulk layer. TN was used in pocket calculators, wrist watches, and later note PCs and monitors. However, TN is outdated because of its poor contrast ratio and strong viewing angle dependency. Great improvement of the viewing angle was achieved with in-plane switching (IPS)[6] or fringe field switching (FFS) modes.[7] Another decisive advantage of these modes is their lack of optical response towards variations in the layer thickness, caused, for example, by mechanical pressure. This renders IPS/FFS LCDs particularly well-suited for touch panels, which have become a key component of smartphones and tablet PCs. Interdigitated electrodes are located at only one side of the cell and generate an in-plane electric field. The LC molecules align with the field and rotate in-plane, thus leading to a better viewing angle. However, LC molecules just above the electrodes do not rotate in-plane, but tilt out of it, thereby giving rise to somewhat deteriorated optical appearance. Therefore, a so-called black matrix is used to cover these regions, at the price of lower aperture ratio in IPS/FFS panels. This drawback can be overcome by a wider distance between the interdigital electrodes. Since the total available voltage is limited due to power consumption, this should be compensated by higher dielectric anisotropy of the LC materials. Thus, the most important task in the development of LC materials is to identify novel LC materials with a favorable combination of high dielectric anisotropy ($\Delta\varepsilon$), low rotational viscosity (γ_1), good solubility, and a broad nematic phase range.

Dielectrically negative materials were first considered for the so-called electrically controlled birefringence (ECB) mode,[8] where the high sensitivity of transmission–voltage curves to the wavelength of the light can allow control over the generation of color. Thus, it is in principle possible to obtain colors by applying the corresponding voltage. Practical difficulties, especially with the surface orientation of the liquid crystals together with the poor voltage holding properties of the materials available at the time, seriously hindered the development of this technology. However, in the mid-1990s, careful optimization[3] of the material parameters led to mixtures that could be employed in the first multidomain vertical alignment (MVA) displays[9] made by Fujitsu in Japan. MVA solved the alignment problem of ECB, and the multidomain structure led to good dependence on the viewing angle. Desktop monitors based on MVA became commercially available in the late 1990s. MVA was further developed and refined at Sharp[10] (advanced superview, ASV) and Samsung[11] (patterned vertical alignment, PVA). More recently, photoalignment and in-cell polymer-based alignment techniques have been developed for dielectrically negative materials (see Section 8.1.), and are now on their way to supersede the older alignment methods. The main advantages of all VA modes are their enhanced black state, which give high contrast and better viewing angle dependence, and their fast response time. The former point in particular turned out to be decisive for the technological breakthrough of LCD televisions.

For display applications, the absolute value of the dielectric anisotropy $\Delta\varepsilon$ should be large to decrease the operating voltage towards lower power consumption. The rotational viscosity γ_1 should be as low as possible to allow fast switching, and the birefringence Δn has to be adjusted to fit the precise display configuration, in particular the cell gap.

A suitable set of properties cannot be achieved with a single material; instead a mixture of typically 10–15 compounds has to be optimized to fulfill the requirements of the LCD manufacturers. In current premium LCD TVs, VA technology has assumed the leading role, followed by the IPS/FFS mode. Less-expensive TV models also employ conventional TN displays.

3. Difluoroether-Based Liquid Crystals for IPS/FFS Technology

Initially, the use of fluorine substitution in liquid crystals was limited mainly to aromatic moieties and to short, fluoroaliphatic polar terminal groups. As a part of a systematic program exploring the full range of structural possibilities, several fluoroaliphatic "bridge" elements between nematogenic rings—in particular CF_2O[12] and CF_2CF_2[13] bridges—were investigated towards the end of the 1990s. The targeted property profile was a combination of high dielectric anisotropy ($\Delta\varepsilon$), low rotational viscosity (γ_1), good solubility, and a broad nematic phase range.

As a consequence of the inconvenient synthetic access,[14] only a very limited set of liquid crystals containing the CF_2O substructure was synthesized and characterized initially, which yielded no interesting candidates for further study. Starting from around 1999, several new synthetic routes were developed, thereby enabling access to gram-scale quantities of liquid crystals with the difluorooxymethylene moiety at all relevant positions of the mesogenic core structure, and allowing a systematic evaluation of the substance class for the first time (Scheme 2).[15] However, these synthetic protocols often require expensive chromatographic purification procedures.

The breakthrough synthetic approach to difluoroether-based liquid crystals on an industrial scale at an economically feasible cost employs the oxidative fluorodesulfuration of dithianylium salts.[16] The dithianylium salts can be either isolated or they are generated in situ by the protonation of a suitable ketenedithioketal.[17] The reversibility of the protonation step permits the exclusive formation of the desired, thermodynamically preferred, 1,4-trans-disubstituted cyclohexane derivatives (Scheme 3).

It was quickly shown that the CF_2O moiety imparts unique and highly attractive physical properties to materials when it is incorporated between the cyclic subunits of the mesogenic core structure. Depending on its exact location, insertion of the difluoroether bridge often results in a dramatic increase in the clearing temperature, extension of the nematic phase range, and—at the same time—a significant reduction in the rotational viscosity (Table 1). The last point is particularly remarkable, since until then it had been an established design rule that elongation of the mesogenic core structure by insertion of a bridging unit always results in an increase in the rotational viscosity.
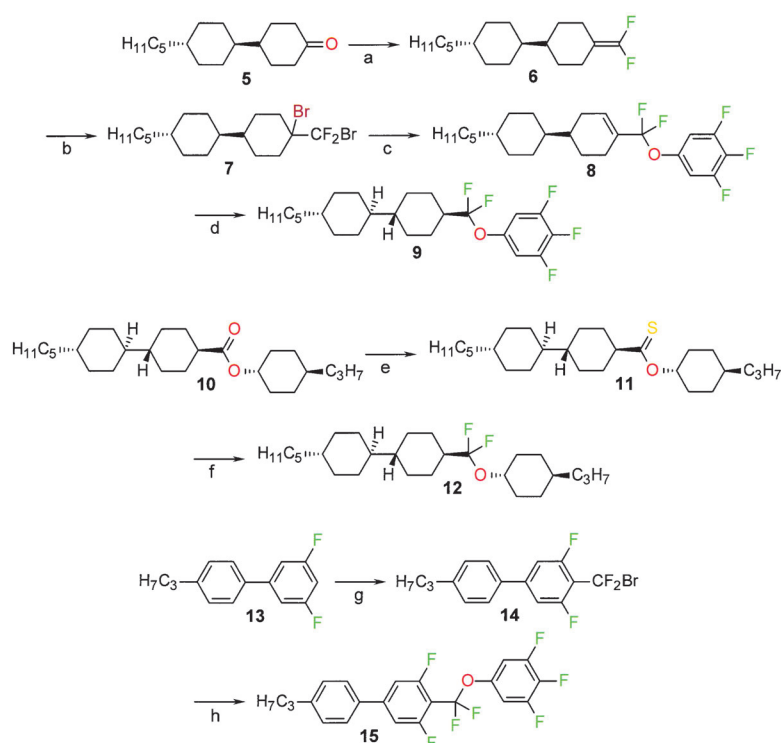
Scheme 2. Various synthetic routes towards liquid crystals containing the CF$_2$O moiety: a) CF$_2$Br$_2$, P(NMe$_2$)$_3$, THF/dioxane; 0°C to RT, 18 h (99%); b) Br$_2$, CH$_2$Cl$_2$; 0°C→RT, 2 h (67%); c) 3,4,5-trifluorophenol sodium salt, DMF; 60°C, 8 h (34%); d) 1. H$_2$, 5% Pd-C, THF; 2. multiple crystallizations from *n*-pentane (3%); e) Lawesson's reagent, toluene; reflux, 3 days (52%); f) DAST, CH$_2$Cl$_2$; RT, 4 h (49%); g) 1. *n*BuLi, THF; −78°C, 1 h; 2. CF$_2$Br$_2$; −70°C→RT, 1 h (65%); h) 3,4,5-trifluorophenol sodium salt, DMEU; 100°C, 6 h (29%). Lawesson's reagent = 2,4-bis(4-methoxyphenyl)-1,3,2,4-dithiadiphosphetane-2,4-dithione, DAST = diethylaminosulfur trifluoride, DMEU = 1,3-dimethyl-2-imidazolidinone.
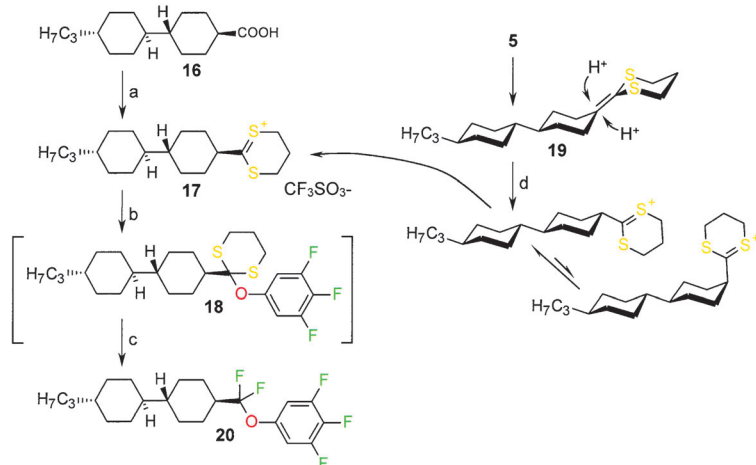
Scheme 3. Synthesis of the liquid crystal 20: a) 1. HS(CH$_2$)$_3$SH, CF$_3$SO$_3$H, toluene/2,2,4-trimethylpentane 1:1; azeotropic removal of water; 2. crystallization by addition of methyl-*tert*-butyl ether at 0°C (90%); b) 3,4,5-trifluorophenol, NEt$_3$, CH$_2$Cl$_2$; −70°C, 10 min; c) 1. NEt$_3$·3HF; −70°C, 5 min; 2. Br$_2$; −70→0°C (84%). d) CF$_3$SO$_3$H, CH$_2$Cl$_2$; 0°C (5 min) → RT (30 min) → −70°C.

Table 1: The physical property profiles of analogues of **21** with various fluorine contents in the bridge structure.[18]

	X	Y	Mesophase sequence	T_{NI}	$\Delta\varepsilon$	Δn	γ_1
20	F	F	C 44 N 105.3 I	91.5	10.5	0.0668	145
21	H	H	C 84 N (78.5) I	65.7	8.3	0.0759	357
22	H	F	C 43 N 88.0 I	75.6	8.0	0.0659	300
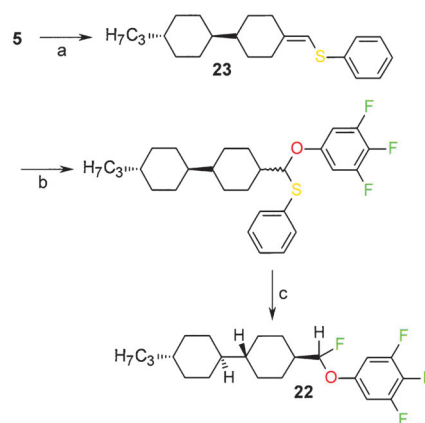
Scheme 4. Synthesis of **22**: a) Ph$_3$PCH$_2$SPh$^+$Cl$^-$, KO*t*Bu, THF; −10°C (48%); b) 3,4,5-trifluorophenol, cat. CF$_3$SO$_3$H, CH$_2$Cl$_2$; 0°C, 1 h (crude product used without further purification); c) 1. NEt$_3$·3HF; −70°C, 5 min; 2. DBH; −70°C→RT (37%). DBH = 1,3-dibromo-5,5-dimethylhydantoin.

What are the reasons behind these unexpected "bridge" effects? To confirm whether the effect is related to the presence of fluorine, the non- (**21**) and mono-fluorinated (**22**) analogues of **20** were prepared (Table 1 and Scheme 4).

First of all, a comparison of the physical properties of directly linked **3** with the nonfluorinated ether-bridged congener **21** confirms the old design rule: the virtual clearing point drops and the rotational viscosity increases. However, the stepwise introduction of fluorine into the bridge results in an increase in the clearing temperature and an extension of the nematic phase range. At the same time, the rotational viscosity of **21** ($\gamma_1 = 357$ mPas) is reduced significantly by the introduction of even one fluorine atom (**22**: $\gamma_1 = 300$ mPas) and halved by difluorination (**20**: $\gamma_1 = 145$ mPas).

Having established the role of fluorine substitution unequivocally, the question of the mechanism was addressed by a computational study.[19] The conformational space of simple model compounds was examined starting with the working hypothesis that the fluorination enhances the rigidity of the bridge and thus stabilizes the aspect ratio of the nematic liquid crystal. Fluorination increases the energy difference between *anti* and *gauche* conformers of the model compound ethyl methyl ether in favor of the *anti* conformer, which corresponds to an elongated, rodlike conformation of liquid crystals such as

8884 www.angewandte.org

© 2013 Wiley-VCH Verlag GmbH & Co. KGaA, Weinheim

Angew. Chem. Int. Ed. **2013**, *52*, 8880–8896

20. Transferred to the conformational situation in "real" liquid crystals, the stereoelectronic effects work in several ways: Firstly, negative hyperconjugation[20] of the lone pair of electrons on the oxygen atom with the antibonding σ* orbital of the C–F bond (n_O-σ*$_{CF}$) increases the rotational barrier around the central C–O bond from 5.7 to 10.3 kcal mol^{-1}, and the *anti–gauche* equilibrium is shifted towards the more rodlike *anti* conformer. Secondly, negative hyperconjugation of the electron-rich C–H bond at the cyclohexane bridgehead position with the σ* orbital of the C–F bond (σ$_{CH}$-σ*$_{CF}$) provides further conformational stabilization of the bridge against twisting of the cyclohexane moiety. A minor additional stabilization comes from C–C hyperconjugation involving the cyclohexane C–C bonds (σ$_{CC}$-σ*$_{CF}$ hyperconjugation). To get

Table 2: Comparison of the physical properties of pure carbocyclic, highly polar liquid crystals **25** and **26–28**.[18]

	Mesophase sequence	T_{NI}	$\Delta\varepsilon$	Δn	γ_1
25	C 48 I	−20.6	25.2	0.1579	96
26	C 120 I	72.6	14.3	0.238	127
27	C 62 N (27.6) I	36.8	19.6	0.2187	153
28	C 108 I	0.9	23.4	0.2091	177

a more quantitative impression of the order of magnitude of these different stereoelectronic effects, the n_O–σ*$_{CF}$ interaction provides ca. 19–20 kcal mol^{-1} of electronic energy, σ$_{CH}$–σ*$_{CF}$ hyperconjugation ca. 6.7 kcal mol^{-1}, whereas σ$_{CC}$–σ*$_{CF}$ hyperconjugation gives only around 3.5 kcal mol^{-1}. Crystal structures of CF$_2$O-bridged liquid crystals[21] (for example, **24**) show an optimal alignment for these interactions (Figure 1).
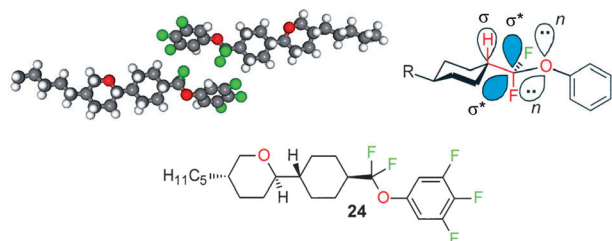
direction of the long molecular axis, thus increasing the dielectric anisotropy.

In highly fluorinated materials such as **29** (the ethyl homologue of **25**), the crystal structure is very much dominated by the complementary charge distribution between nonfluorinated and highly fluorinated aromatic moieties (Figure 2).
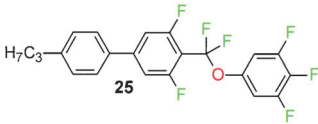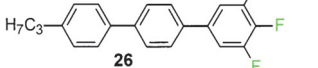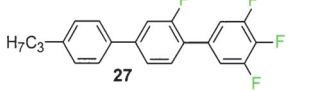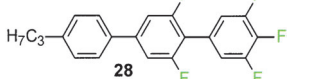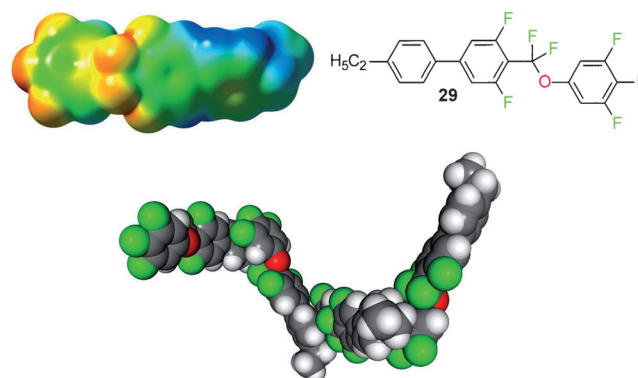

Figure 1. Crystal structures (top left, for example **24**) as well as theoretical analysis both show an orbital alignment (top right) which is optimal for a torsional rigidification of the CF$_2$O bridge.[19]

Apart from the partially cycloaliphatic liquid crystals of type **20**, materials containing only aromatic moieties in their mesogenic core (**25**) are critical components of commercial liquid-crystal mixtures. The main application areas of these materials are in-plane switching (IPS) and fringe field switching (FFS) LCDs for touch panels, as they have become ubiquitous in smartphones and tablet PCs. The aromatic compounds, such as **25**, do not show wide nematic mesophases such as, for example, **20** (Table 2).

Their decisive advantage is the combination of high polarity with low rotational viscosity and good solubility. Highly polar terphenyl-based liquid crystals of the previous generation of materials often suffer from poor solubility, which tends to get worse with increasing fluorine content. On the other hand, aromatic fluorination is required to obtain a sufficient dielectric anisotropy of the material. This limitation of fluorination can be overcome by the solubilizing effect of the inserted CF$_2$O bridge. In addition, the CF$_2$O bridge contributes to the molecular dipole moment in the

Figure 2. The electrostatic potential surface of **29** (top left; blue denotes positive, red negative partial charges) and its crystal structure (bottom). The packing is dominated by the electrostatic attraction between highly fluorinated and nonfluorinated arene moieties, which exhibit complementary charge profiles.
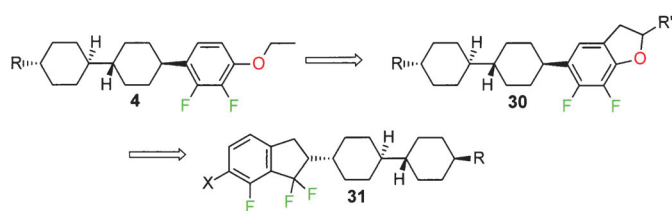
As a consequence of their unique property profiles, difluorooxymethylene-bridged liquid crystals such as **20** or **25** have become a key component in most IPS/FFS mixtures for touch panels and LCD TVs, as well as in TN LCDs for inexpensive TV sets, desktop PC monitors, and notebook PCs.

4. Fluorinated Indane Derivatives for Vertical Alignment

The synthesis and properties of materials with negative dielectric anisotropy, such as **4** and many more structures

containing an *ortho*-difluorophenyl ring, were first published in 1989. Based on studies by Gilman and Bebb[22] as well as Wittig and Fuhrman,[23] the "directed *ortho*-metalation" (DOM) chemistry later developed by the Snieckus research group[24] was key to a series of patent applications and scientific papers.[25] Since then, many attempts have been made by several research groups to improve the materials, for example, increasing the polarity by the introduction of more oxygen substituents next to the fluorine atoms[26] or with heterocyclic rings such as pyridine,[26] pyridazine,[27] and, more recently, tetrahydropyran.[28] Another approach is the introduction of axial polar substituents in cyclohexane rings, highly fluorinated lateral substituents on the aryl rings, or the replacement of the aliphatic rings by aromatic rings to give oligophenyls, and, of course, combinations of these strategies.[4] Instead of the benzene moiety, fluorinated naphthalenes[29] have also been used as polar ring elements for VA-type liquid crystals.

Another, perhaps more subtle idea to increase the polarity of structures such as **4**, is to freeze the rotation around the carbon–oxygen bond by incorporating the oxygen atom into a five-membered ring (**30**; Scheme 5). Dihydrobenzofurans
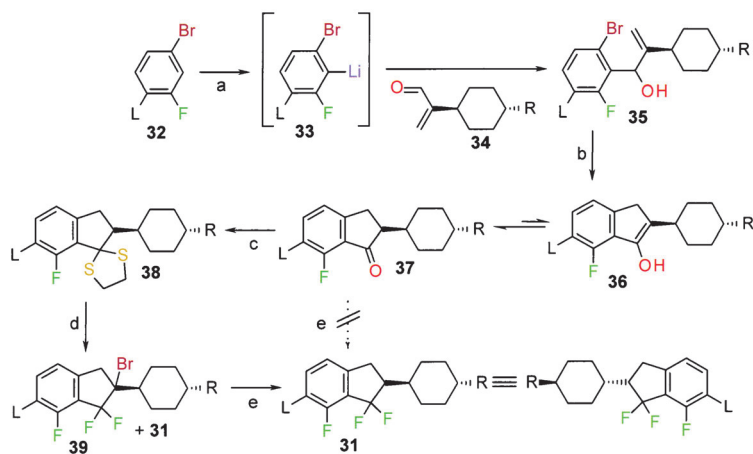
Scheme 6. The synthesis of tri- and tetrafluoroindanes **31** (L=H or F): a) 1. LDA, THF; −70°C; 2. aldehyde **34** (75%); b) cat. [(*o*-Tol₃P)₂PdCl₂], NEt₃, MeCN; reflux (65%); c) HSCH₂CH₂SH, BF₃·OEt₂, CH₂Cl₂; −15°C→RT (80%); d) DBH, HF·pyridine, CH₂Cl₂; −65°C (85%); e) 1. DBU, CH₂Cl₂; RT; 2. H₂, 5% Pd-C (80%). DBH = 1,8-diazabicyclo[5.4.0]undec-7-ene., LDA = lithium diisopropylamide.

Scheme 5. Design of polar, dielectrically negative liquid crystals using conformational restriction (X = H or F).

30 and the corresponding benzofurans were synthesized, but their overall properties were a disappointment.[30] The initial goal, namely to increase the polarity, was achieved, but at the expense of other important properties such as the clearing temperatures and the viscosity. The latter are determined by condensed-phase phenomena and cannot be easily predicted by semirational arguments based on chemical intuition.

With hindsight, the substitution pattern in the dihydrobenzofuran materials **30** was less than ideal: the substituent R′ in the saturated five-membered ring points out of the plane of the ring system and probably causes the low clearing points and high viscosities. The situation is different with the planar benzofurans, but here the polarity is not enhanced over that of the open-chain system. The reason is the incorporation of the density from the lone pair of electrons of the oxygen atom into the aromatic π system, thereby leading to a reduction of the dipole moment. Turning the (hetero)indane system of **30** around and replacing the ring oxygen atom by a *gem*-difluoromethyl group can solve both of these problems (**31**; Scheme 5).

The synthesis of trifluoro- and tetrafluoroindanes[31] (Scheme 6) was considered straightforward: The regiochemistry was controlled by an *ortho*-metalation step between the
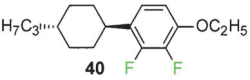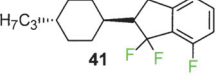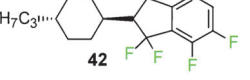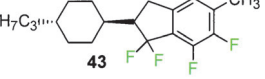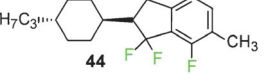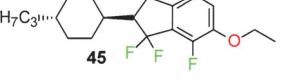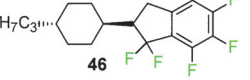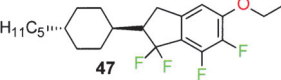
fluorine and bromine substituents at the 1,3-positions of an aromatic ring. The lithiated intermediate **33** was then treated with an α,β-unsaturated aldehyde **34** to form an allylic alcohol **35**. The cyclization step proceeds through an intramolecular Heck reaction, with the allylic double bond attacking the bromine atom to form indanone **37**. This was then expected to be converted directly into the desired germinal difluoroindane **31**. Unfortunately, the rest of the synthesis turned out to be much more difficult than anticipated, as a direct conversion of **37** into **31** was not feasible: When a variety of established fluorination methods was used,[32] the reaction either did not proceed or—when forcing conditions and more reactive reagents were employed—black tars were obtained and no product could be isolated. It was, therefore, necessary to follow an indirect approach by an oxidative desulfurization/fluorination sequence.[33] Again, no clean reaction of **38** to **31** was obtained, but significant amounts of bromine-containing side products **39** were formed, and additional elimination and hydrogenation steps were necessary. The unsaturated aldehydes **34** used in the 1,2-addition must be aliphatic, since the aromatic variants give hetero-Diels–Alder dimers even at room temperature. The fluorinated indanes could be further functionalized at the aromatic ring by *ortho*-metalation. In the end, instead of the short three-step synthesis originally envisioned, a rather cumbersome six-step sequence had to be followed (Scheme 6).

The first fluorinated indane made was **41**, which contains only one aromatic fluorine atom (Table 3). The compound as such is not a liquid crystal: It melts at 100.0°C to an isotropic liquid. This is in fact not uncommon for materials used in commercial LC mixtures. Of interest for practical applications is the effectiveness of the new material when it is dissolved in a nematic liquid-crystalline matrix, the so-called host. This influence is easy to check by measuring the effect of the dissolved compound at a defined concentration on the physical properties of the host liquid-crystal mixture. Data for the single compound can then be estimated by extrapolation to a concentration of 100%.[18]

Table 3: Properties of fluorinated indanes compared to **40**.[18]

	Mesophase sequence	T_{NI}	$\Delta\varepsilon$	Δn	γ_1
40	C 60 I	−15.1	−5.4	0.106	112
41	C 100 I	18.1	−6.7	0.086	136
42	C 85 I	49.4	−8.6	0.085	142
43	C 90 I	48.7	−9.9	0.084	221
44	C 102 I	78.3	−6.9	0.089	157
45	C 104 I	112.6	−10.5	0.094	284
46	C 72 I	38.1	−2.3	0.085	141
47	C 129 I	40.0	−13.5	0.091	514

The polarity of **41** increases to $\Delta\varepsilon = -6.7$, compared to −5.4 for the reference material **40**. At the same time, the clearing point is raised by more than 30 °C to 18.1 °C, but the rotational viscosity increases only slightly. Rotational viscosities usually show a correlation with the clearing temperatures, which are in turn related to the length of the calamitic molecule. Increasing the polarity without sacrificing the clearing point or viscosity is a rather uncommon but very attractive change in the properties.

Introducing a fourth fluorine atom yields **42**, and the phenomena discussed for **41** are repeated: The polarity and clearing points increase, but the viscosity remains essentially the same. An additional methyl substituent increases the polarity again, but now at the expense of the clearing point and viscosity. The birefringence of the new indanes is slightly lower than that of **40**.

In general, substituents at the 6-position of the indane system appear to increase the clearing point. With a methyl group in **44**, the clearing temperature rises to 78 °C, and with the ethoxy group in **45** up to 113 °C. A fifth fluorine atom in **46** deteriorates the properties as expected: The polarity drops to $\Delta\varepsilon = -2.3$, which is too low to make such a material attractive. On the other hand, a record polarity of $\Delta\varepsilon = -13.5$ is achieved in **47**, but now the rotational viscosity is also quite high.

Another way to further increase the polarity is the introduction of a tetrahydropyranyl (THP) ring instead of the simple cyclohexane. This complicates matters somewhat as the presence of a third stereocenter in the molecule ring now opens the possibility of the formation of diastereomers. One of those diastereomers, **48**, should exhibit increased polarity, while the other one, **49**, should be of lower polarity
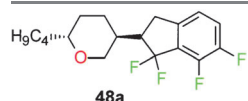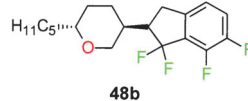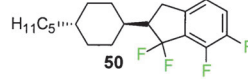
(Scheme 7). The synthesis is analogous to the standard route shown in Scheme 6; only the α,β-unsaturated aldehyde contains the tetrahydropyranyl ring, and it was synthesized as a racemic mixture in seven steps from the corresponding δ-lactones (Scheme 8).

Two different homologues of **48** were synthesized (**48a**: R = C₄H₉, **48b**: R = C₅H₁₁), each one in 13 steps, and in both cases the more polar diastereomer was the only isolated product (Table 4).[34] Compared to **50**, the dielectric anisotropy values $\Delta\varepsilon$ of the new compounds **48a** and **48b** were twice as high! The calculated $\Delta\varepsilon$ value for **48a** is −12.1 at the AM1 level of theory. This compares to a calculated value of −6.5 for carbocyclic **50**. In general, the calculations on the fluorinated indanes yield $\Delta\varepsilon$ values which are too low when compared to experiment. Going to higher levels of theory does not improve the predictions. However, the calculations
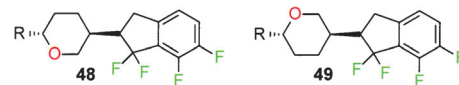
Scheme 7. Possible diastereomers **48** and **49** of difluoroindane-based liquid crystals containing an additional tetrahydropyran (THP) moiety.
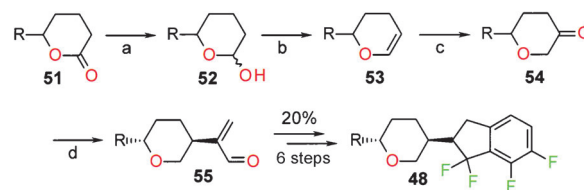
Scheme 8. Synthesis of the tetrahydropyran-containing tetrafluoroindane **48**: a) DIBAL, toluene (85%); b) MsCl, NEt₃, cat. DMAP (70%); c) 1. BH₃·THF; 2. PCC (60%); d) 1. MeOCH=PPh₃/THF; 2. aq HCl; 3. cat. NaOH, MeOH; 4. MeOCH=PPh₃, THF; 5. aq HCl; 6. H₂C=NMe₂Cl, CH₂Cl₂, NEt₃; RT (50%). DMAP = 4-dimethylaminopyridine, DIBAL = diisobutylaluminum hydride, MsCl = methylsulfonyl chloride, PCC = pyridinium chlorochromate.

are for isolated molecules in the gas phase. Intermolecular interactions must play an important role in the condensed liquid-crystalline phase. An indication of this is found in the crystal structure of **43**. The molecules are oriented with the dipole moments aligned in parallel. However, the presence of an inversion center in the space group ($P\bar{1}$) leads to an overall macroscopic dipole moment of zero. In the less strictly ordered nematic phase and in an electric field, this association might lead to the observed enhanced dielectric anisotropy.

Table 4: Properties of THP-containing tetrafluoroindanes.[18]

	Mesophase sequence	T_{NI}	$\Delta\varepsilon$	Δn	γ_1
48a	C 70 I	8.6	−15.8	0.081	326
48b	C 79 I	20.5	−15.6	0.086	360
50	C 74 N (64) I	60.3	−7.8	0.077	116

These results suggest that intermolecular interactions among fluorinated compounds influence the properties of the condensed phase in ways not yet fully understood and exploited (Figure 3).
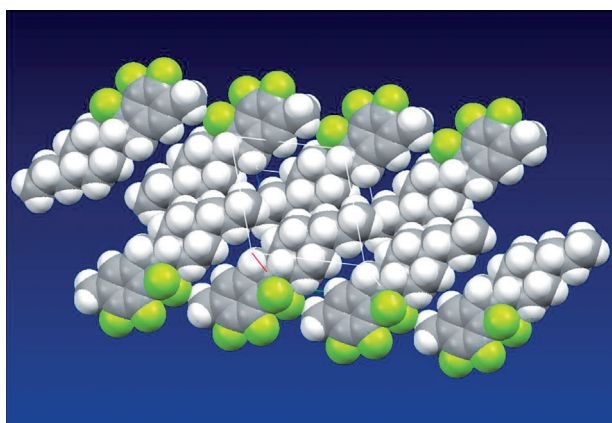

Figure 3. The crystal packing of **43** in the solid state shows regions of parallel molecular alignment.[31]

5. Tetrahydropyran-Based Liquid Crystals

Liquid crystals containing a tetrahydropyran (THP) subunit have been a synthetic target since the early 1990s.[35] THP is an interesting building block because it has an intrinsic dipole moment, which can be utilized to increase the polarity of dielectrically positive as well as negative materials (see, for example, **50**). Moreover, since the 2,6-disubstituted THP unit is chiral, the racemic mixture—which is in fact a eutectic—can be expected to induce a significantly higher solubility to the resulting liquid crystal than, for example, the frequently used 1,3-dioxane subunit.[36] The first synthetic sources for THP came from the chiral pool (e.g., carbohydrates) and resulted in enantiopure chiral liquid crystals, which are normally only used as additives[37] but not for mainstream applications. Later on, several alternative synthetic approaches were developed,[38–40] thus facilitating the access to racemic THP derivatives in general.

Thus, the first racemic, THP-based liquid crystals became available for characterization.[41] Two examples of the synthetic methods used are shown in Schemes 9 and 10. Nowadays, THP derivatives are an important component of liquid-crystal mixtures used in touch panels for smartphones and table PCs.[42]

The polarity ($\Delta\varepsilon$) of the THP derivatives lies between their cyclohexane and the dioxane analogues (Table 5). A major advantage of the THP-based liquid crystals is their high solubility. Integration of a THP subunit renders even highly polar five-ring structures sufficiently soluble in typical
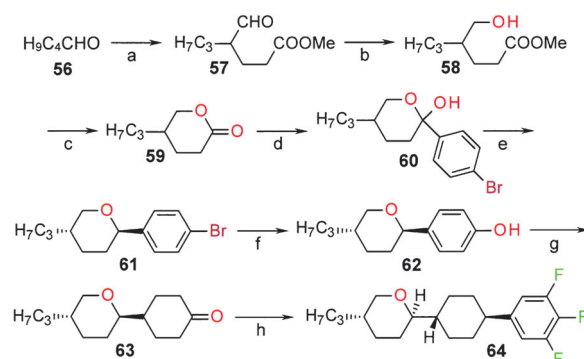
Scheme 9. Synthesis of tetrahydropyran derivative **64** by the δ-valerolactone route: a) 1. Methyl acrylate, Et₂NSiMe₃, CH₃CN; reflux, 18 h; 2. HOAc, H₂O; reflux, 18 h (68%; crude product used for subsequent step); b) NaBH₄, 2-propanol; RT, 18 h (87%); c) 1. cat. *p*-TsOH, toluene; reflux with azeotropic water removal; 2. distillation (61%); d) 1,4-dibromobenzene, *n*BuLi, Et₂O; −50°C (2 h) → −10°C (crude product used for subsequent reaction); e) 1. BF₃·OEt₂, Me₃SiH, CH₂Cl₂; −70°C (2 h) → −10°C (44%); 2. AlCl₃ (0.2 equiv), CH₂Cl₂; −20°C, 30 min (95%); f) 1. *n*BuLi, THF; −70°C (2 h); then B(OMe)₃; −70°C (2 h) → −10°C; 2 N HCl (75%, crystallized from *n*-hexane); 2. 30% H₂O₂, H₂O, HOAc, THF; RT, 6 h (89%); g) H₂, 5% Pd-C, xylene; 5 bar, 120°C (75%); h) 1. 1-bromo-3,4,5-trifluorobenzene, 2-PrMgCl, THF; RT, 1 h; then **63**; RT, 1 h; 2. MeSO₂Cl, NEt₃, CH₂Cl₂; 0°C→RT, 18 h (45%); 3. H₂, 5% Pd-C, THF; 1 bar, RT (60%). TsOH = *p*-toluenesulfonic acid.
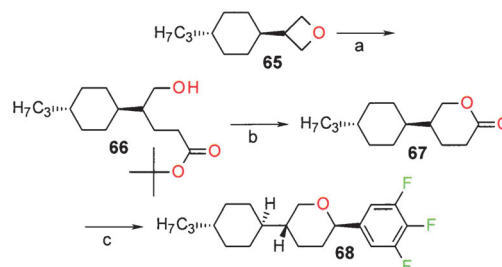
Scheme 10. Synthesis of the liquid crystal **68** by the ring opening of oxetane **65** as a key step: a) *t*BuOAc, LDA, THF; −78°C, 25 min; then **65**, BF₃·OEt₂; −78°C (1 h), then RT (27%); b) CF₃COOH, CH₂Cl₂; RT, 18 h (81%); c) 1. LiPhF₃, Et₂O; −70°C (2 h), then RT (85% crude); 2. BF₃·OEt₂, Me₃SiH, CH₂Cl₂; −70°C (2 h) →−10°C (54%).

8888 www.angewandte.org

© 2013 Wiley-VCH Verlag GmbH & Co. KGaA, Weinheim

Angew. Chem. Int. Ed. **2013**, *52*, 8880–8896

Table 5: Comparison of various THP-based liquid crystals (**64**, **68**) with their purely carbocyclic (**3**) and their 1,3-dioxane analogues (**69**, **70**). Materials **71**–**74** demonstrate the influence of the position of the THP unit within the mesogenic core structure.[18]


	X	Y	Mesophase sequence	T_{NI}	$\Delta\varepsilon$	Δn	γ_1
3	CH₂	CH₂	C 66 N 94.1 I	74.3	9.7	0.0750	160
64	CH₂	O	C 74 I	32.4	15.0	0.0744	136
69	O	O	C 91 I	16.0	21.8	0.0760	226
68	CH₂	O	C 57 N (52.2) I	63.6	12.7	0.0778	–
70	O	O	C 74 N (51.2) I	63.2	17.0	0.0680	201
71	-	-	C 35 N 66.3 I	58.1	14.0	0.0654	158
72	-	-	C 58 N (39.8) I	41.5	12.4	0.0751	–
73	-	-	C? 7 S$_B$ 15 I	−77.8	10.5	0.0483	76
74	-	-	C 59 I	−57.6	8.8	0.0606	–

liquid-crystal mixtures. This opens the way to new classes of super-polar liquid crystals as they find their use in newer display applications such as the blue-phase LCD (Table 6).

Table 5 also shows another effect which comes into the play if a THP unit and an electronegative polar group are direct neighbors: in these cases all indicators of anisotropy (occurrence of mesophases, T_{NI}, $\Delta\varepsilon$, Δn) show a significant drop compared to the analogous compounds where THP and the polar group X (typically CF₃ or CF₂O-aryl) are separated by a cyclohexane unit. For example, in the pairs **71/72** and **73/74** with their electronegative CF₂OR or CF₃ moieties, **72** and **74** have significantly less-pronounced mesogenic characteristics. This effect had thus far not been noticed in liquid crystals. Presumably, it is a stereoelectronic conformation effect, which is related to the anomeric effect well-known in carbohydrates:[43] The overlap of the axial oxygen lone pair of electrons with the antibonding (σ*) orbital of the neighboring C–X bond stabilizes the axial arrangement of the substituent X with increasing electronegativity of X. The thus stabilized axial-axial conformation results in a "kink" in the liquid-crystal molecule, thereby rendering it less "rodlike", that is, decreasing its length/breadth ratio (Scheme 11).

Although the racemic THP derivatives are mainly of interest for application in LCDs, enantiomerically pure samples were also prepared to evaluate their potential as
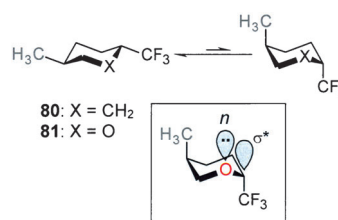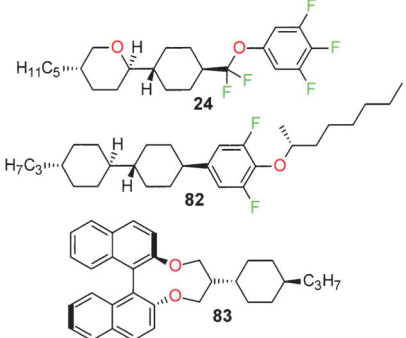
Scheme 11. The influence of the anomeric effect on the conformational equilibrium of liquid-crystalline tetrahydropyran derivatives: In the cyclohexane-based system **80** the bis-equatorial conformer is energetically preferred by 4.5 kcal mol⁻¹, for the THP system **81** only by 2.7 kcal mol⁻¹ (calculated on the MP2/6-311+G(2d,p)//B3LYP/6-31G(d)+ZPE level of theory).[44]

Table 6: Examples of super-polar liquid crystals with four or five rings and containing a THP moiety.[18]

	Mesophase sequence	T_{NI}	$\Delta\varepsilon$	Δn	γ_1
75	C 83 N (83.0) I	56.4	35.6	0.1316	457
76	C 74 S$_C$ (67) N 144.8 I	87.7	66.6	0.1568	1016
77	C 98 N 193.0 I	134.7	37.1	0.1544	1225
78	T_g −14 C 96 N 240.6 I	167.3	70.3	0.1827	–
79	C 127 S$_A$ 212 N 251.1 I	212.4	35.6	0.1353	–

Table 7: The physical properties of racemic and enantiopure liquid crystal 24 in comparison with typical chiral dopants.[45][a]

No.	Mesophase sequence[a]	$[\alpha]_D^{20}$	HTP
rac-24	C 39 N 75.3 I	–	–
D-24	C 41 N* 73.3 I	+4.5	+0.8
L-24	C 42 N* 74.3 I	−4.9	−0.8
82	C 19 S_B 45 N* 72 I	–	−13.6
83	C 161 I	–	−85.1

[a] The optical rotations are cited in °, and the helical twisting power (HTP) in μm^{-1}; C = crystalline, N = nematic, N* = chiral nematic (cholesteric), I = isotropic. The HTP was measured in the nematic host mixtures MLC-6012 (82) and MLC-6260 (24, 83).

chiral dopants. However, D- and L-24 showed a surprisingly low helical twisting power (HTP), which is far below the performance of commonly used chiral dopants (Table 7).

6. Hypervalent Sulfur Fluorides as Super-Polar Terminal Groups

The reduction of production cost has become a major technology driver in the strongly competitive environment of a saturating market for LCD TVs. Another driving force is the demand for ever-faster response times to improve the picture quality as well as to enable 3D TV with a rate of 48 frames per second. For both of these seemingly unrelated demands, LCDs based on the so-called blue phase[46] are currently considered as an attractive solution (see Section 8.2).

The blue phase can be switched very quickly (< 1 ms) and, because of its optical isotropy, it does not require an expensive alignment layer. The liquid-crystal mixture needs to have an extremely high $\Delta\varepsilon$ value in combination with a good voltage holding ratio (VHR). One promising strategy towards this goal is the use of fluorinated, super-polar terminal groups. Ideally, the dipole moment of such a group should exceed that of the trifluoromethyl group. One candidate to address this rather extreme technical requirement is the λ_6-pentafluorosulfanyl (SF$_5$) group. Although this functional group has been known since the early 1960s,[47] the rather inconvenient synthetic access impeded further experimental study for the subsequent 40 years. Compared to the trifluoromethyl group, the pentafluorosulfanyl group is more polar (the dipole moment μ of pentafluorosulfanylbenzene is 3.44 D, compared to 2.60 D for trifluoromethylbenzene), but is sterically more demanding and more lipophilic. In 1996,

pentafluorosulfanyl arenes became commercially available by a direct fluorination process,[48] and in 2008, a further improved process was developed by using chlorine in combination with a fluoride source for the oxidation step (Scheme 12).[49]
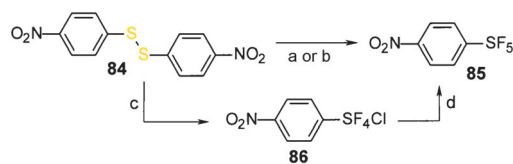
Scheme 12. Synthesis of pentafluorosulfanyl arenes: a) 1. AgF$_2$, CFC-113; 80°C, copper autoclave; 2. 120°C (16%); b) 10% F$_2$-N$_2$, CH$_3$CN; −7.6→−4.5°C, 24 h (41%); c) Cl$_2$, KF, CH$_3$CN; 0°C, 3 h (88%); d) ZnF$_2$; 120°C, 2 h (89%). CFC-113 = 1,1,2,-trichloro-1,2,2-trifluoro-ethane.

Another route towards aromatic as well as aliphatic SF$_5$ derivatives is based on the radical addition of SF$_5$Cl or SF$_5$Br to olefins.[50] However, the SF$_5$Cl and SF$_5$Br reagents have never been commercially available on a large scale.

Chemically, the SF$_5$ group is highly stable and comparable to the trifluoromethyl group. This has been demonstrated in the 1960s by Sheppard and co-workers, and similar synthetic methodology was applied in 1999 for the synthesis of the first liquid crystals containing a pentafluorosulfanyl group.[51] In 2006, several non-aromatic materials with an SF$_5$ substituent were also reported (Scheme 13).[50f]
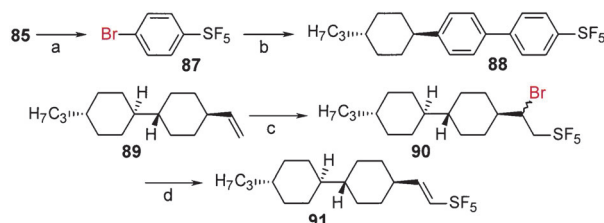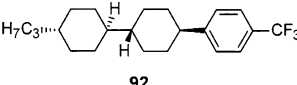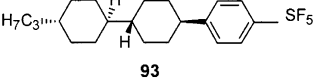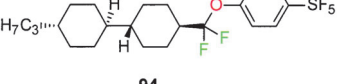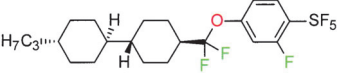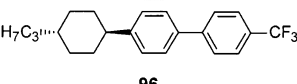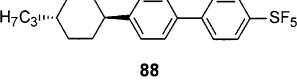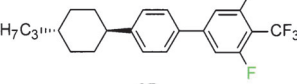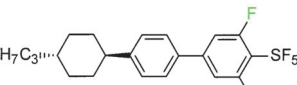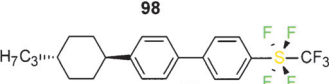

Scheme 13. Synthesis of the first liquid crystals (88) containing an SF$_5$ terminal group (top). Cycloaliphatic liquid-crystalline SF$_5$ derivatives (90) are also accessible by using SF$_5$Br as the pentafluorosulfanylation reagent (bottom): a) 1. H$_2$, 5% Pd-C, THF; 1 bar, RT (100%); 2. aq HBr, NaNO$_2$; −5°C; 3. CuBr; RT→80°C (46%); b) 4-(4-propylcyclohexyl)benzeneboronic acid, cat. [Pd(PPh$_3$)$_4$], toluene, 2 N NaOH; RT, 2 days (23%); c) SF$_5$Br, BEt$_3$ (0.15 equiv), n-heptane; −40→−20°C, 2 h (85%). d) KOH powder, n-heptane; 35°C, 18 h (74%).

As expected, SF$_5$-based liquid crystals show a higher dielectric anisotropy than their CF$_3$ analogues. As a consequence of the weak interaction of the pentafluorosulfanyl group with ionic impurities in the LCD, the materials show an excellent voltage holding ratio. However, presumably because of its steric bulk, the SF$_5$ group induces very high rotational viscosity (γ_1) in the liquid crystal (Table 8).

Since the main advantage of the pentafluorosulfanyl group is its polarity, several approaches were taken to further increase the dielectric anisotropy ($\Delta\varepsilon$) of the SF$_5$-based liquid crystals. Different mixture concepts might become applicable for even more polar materials, thus rendering the high γ_1 value of the SF$_5$ derivatives less critical. The conventional

8890   www.angewandte.org

© 2013 Wiley-VCH Verlag GmbH & Co. KGaA, Weinheim

Angew. Chem. Int. Ed. 2013, 52, 8880–8896

Table 8: Physical properties of SF$_5$-based liquid crystals in comparison with their trifluromethyl analogues and some other materials with similar polarity.[18]

	Mesophase sequence	T_{NI}	$\Delta\varepsilon$	Δn	γ_1
92	C 133 I	112.2	9.5	0.0910	338
93	C 121 I	95.5	11.6	0.0933	612
94	C 67 N 116.5 I	108.2	11.8	0.0800	488
95	C 50 N 101.9 I	87.6	14.3	0.0801	–
96	C 134 I	108.6	13.0	0.1645	279
88	C 109 N (87.8) I	94.6	14.3	0.1537	634
97	C 86 I	47.1	21.5	0.1490	–
98	C 103 I	49.6	21.4	0.1319	–
99	C 197 N 209.7 I	182.6	10.6	0.1499	–

approach to increase the polarity of liquid crystals is to substitute the aromatic *ortho* positions of the polar terminal group with fluorine.[52] Typically, this results in an increase in the $\Delta\varepsilon$ value by about 8 units (e.g. **96**→**97**). In the case of the SF$_5$ group, early computational studies indicated that this effect might be even more pronounced, because the *ortho*-fluorine substituents were presumed to push the "belt" of equatorial fluorine atoms of the octahedral SF$_5$ group forward into the direction of the long molecular axis, thus enhancing the group dipole moment significantly. However, *ortho*-fluorinated materials failed to show the desired high $\Delta\varepsilon$ value because of the easy deformability of the SF$_5$ group: the equatorial fluorine atoms were not pushed "forward" as expected, but were pushed apart, with the *ortho*-fluorine atom inserted between them and resulting in a slight "backward" shift with a partial compensation of the group dipole moment.

A second strategy to increase the polarity of the penta-fluorosulfanyl group is based on its octahedral geometry: whereas the four equatorial fluorine atoms mainly cancel their local S-F$_{eq}$ dipole moments, the axial S-F$_{ax}$ dipole is oriented fully into the direction of the long molecular axis, thus contributing fully to the overall dielectric anisotropy

($\Delta\varepsilon$). Replacement of the axial fluorine atom by a more electronegative group, such as trifluoro-methyl, was expected to increase the overall polarity dramatically. The key step of the synthesis leading to the *trans*-SF$_4$CF$_3$ group[53] is the direct fluorination of 4-trifluoromethylsulfanylnitrobenzene (**100**), which furnishes a mixture of *cis* and *trans* isomers. In a subsequent step, this mixture is isomerized to the thermodynamically preferred *trans* isomer by addition of the Lewis acid AlCl$_3$ (Scheme 14).[54] Just like the SF$_5$ group, *trans*-SF$_4$CF$_3$ is hydrolytically very stable under basic and acidic conditions.

Characterization of the liquid crystal **99** indicated an unexpectedly low dielectric anisotropy $\Delta\varepsilon$—even significantly lower than for the SF$_5$ analogue **88**. The crystal structure of the intermediate *trans*-**101** revealed the cause: the bulky CF$_3$ group pushes the equatorial fluorine atoms "back", thereby inducing local dipoles opposite to the main molecular dipole moment. This results in a partial cancellation, thus reducing the dielectric anisotropy of *trans*-**99**. Therefore, the *trans*-SF$_4$CF$_3$ group cannot be considered a real "super-SF$_5$" group.

The situation can be summarized as a single SF$_5$ group being the most polar of all fluorinated functional groups, and can be truly considered a "super-trifluoromethyl group". However, the ease of sterically induced deformation means that further enhancement of the polarity by either *ortho*-fluorination or axial substitution does not necessarily result in a further increase in the dielectric anisotropy.

The difficulties in enhancing the polarity of liquid crystals with a pentafluorosulfanyl group also illustrate the limits of the computational prediction of properties, which usually allows quite accurate calculation of the electrooptic characteristics ($\Delta\varepsilon$ and Δn) for most materials.[55] For hypervalent sulfur fluorides, standard methods tend to provide quite inaccurate bond lengths and
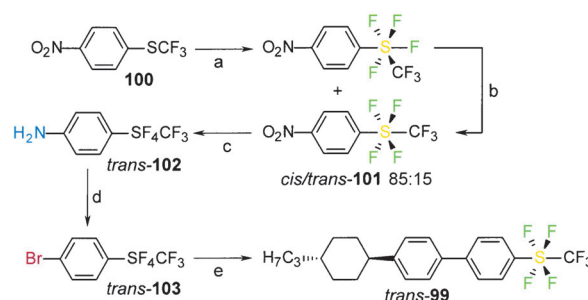
Scheme 14. Synthesis of liquid crystal **99** with a *trans*-SF$_4$CF$_3$ terminal group: a) 10% F$_2$-N$_2$, CH$_3$CN; 0°C (50% isomer mixture, *cis/trans* 85:15); b) AlCl$_3$ (0.8 equiv), CH$_2$Cl$_2$; −10°C, 30 min (48%); c) H$_2$, Raney-Ni, THF; 1 bar (87%); d) 1. 47% aq HBr, NaNO$_2$; 0–5°C; 2. CuBr; 85°C (52%); e) 4-(propyl-4-cyclohexyl)benzeneboronic acid, cat. [Pd(PPh$_3$)$_4$], THF, borate buffer pH9; 85°C, 18 h (14%).

valence angles, thus precluding a reliable prediction of the molecular dipole moment.

7. Reliability

The polarity of the materials presented in the previous sections was mainly generated by fluorine-containing substituents. Other polar groups such as nitriles, esters, and even heterocyclic structures such as pyridines and pyrimidines are no longer used. This is because almost all display applications today are active matrix driven with thin-film transistors (TFTs); only this type of LCD can fulfill the requirements of high information content in combination with good contrast and brightness. A key factor is "reliability", which means that phenomena such as image sticking, where an image "burns in" on the screen after being displayed for a certain time, or so-called mura (Japanese for "clouding") phenomena have to be avoided.

One of the characteristic measurable parameters for reliability is the voltage holding ratio (VHR). VHR is defined as the ratio of the voltages applied to a pixel at the end and the beginning of an addressing cycle.[56] A high VHR is important, since a reduction of the voltage deteriorates the contrast and gives rise to flicker. The VHR is influenced by the resistivity and the capacitance of the AMD cell. The capacitance is mainly related to dielectric properties of the LC and determined by the specification for the operating voltage, that is, the parameter for the improvement is the resistivity.

Possible reasons for low resistivity are the presence of ions or contaminations within the cell that originate from the alignment layers, the liquid crystal itself, or they might even be generated from interactions between the various components. The reliability requirements also depend on the application. TVs are different from monitors because the light sources and resulting display temperatures are very different. Moreover, the change of backlights from cold cathode fluorescent lamps (CCFLs) to light-emitting diodes (LEDs) changed the requirements in terms of the reliability of the LCs since the temperature of the displays is lower and the light spectrum is different with LED backlights. This means that the reliability requirements for LCs are changing frequently, and thus some materials can only be used for certain applications. However, from an LC material design point of view, VHR values are not predictable, but a drop in the VHR indicates a current flow in the cell that can only be explained by the solubilization and mobilization of ion traces by the liquid crystal. Solvation, on the other hand, can easily be modeled through the calculation of ion affinities, for example, to the sodium cation, which is omnipresent in trace amounts (Scheme 15).

As a consequence of the rather modest level of theory employed, the absolute affinity values shown in Scheme 15 might not be reliable—but
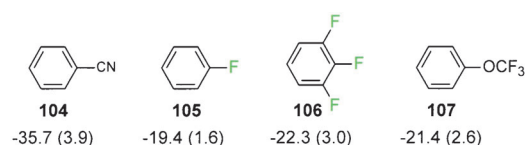
Scheme 15. Calculated sodium cation affinities (kcal mol^{-1}) and dipole moments (in parentheses, Debye) for polar model compounds benzonitrile (**104**), fluorobenzene (**105**), trifluorobenzene (**106**), and trifluoromethoxybenzene (**107**); calculated at the B3LYP/6-311+G(2d,p)//B3LYP/6-31G(d)+ZPE level of theory.[44]

the large difference in affinities between the fluorinated materials **105**–**107** and the "classic" nitrile **104** is clearly visible. It is also interesting to note the absence of a correlation of these affinities with the molecular dipole moments of the organic molecules. 1,2,3-Trifluorobenzene (**106**) is almost as polar as benzonitrile (**104**), but this is not reflected in a necessarily highly negative ion affinity. The fluorinated structures exhibit much lower ion affinities of around −20 kcal mol^{-1}. Polarity alone is clearly not the reason for this difference, it must be the polarizability of the organic molecule that plays an important role.

The response of an organic molecule to the presence of a positive charge can be calculated from the so-called electrostatic potential (ESP). Here, a positive point charge is used to scan the molecule to obtain an isosurface of the potential at a fixed value, typically at −10 kcal mol^{-1}. Figure 4 shows such surfaces for some small model systems. Again, we observe a large difference for the benzonitrile molecule compared to the other model compounds. The volume of the isosurface is more than three times that of the parent benzene molecule. Fluorination decreases the ESP volume when going from benzene (33.6 Å^3) to 1,2,3-trifluorobenzene (29.0 Å^3).

For these reasons, research in the "device chemicals" area now focuses on fluorinated liquid crystals, which combine the necessary polarity with chemical stability and a small propensity for the solvation of ion traces. However, as we have already seen, not only polarity, but also mesophase properties and viscoelastic properties of LCs are mediated in often surprising ways by fluorine substituents.

The design of new materials for LCDs is complicated by negative trade-off property relationships: Higher polarity and

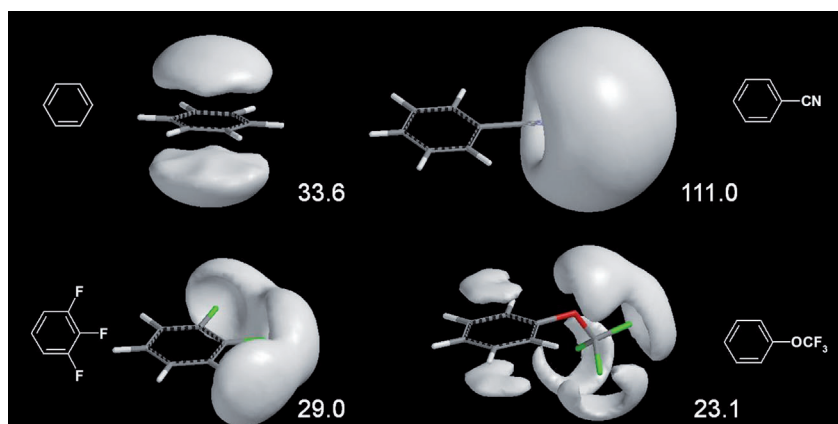**Figure 4.** Electrostatic potential isosurfaces (at −10 kcal mol^{-1}) and their volumes (in Å^3) for model compounds.

8892   www.angewandte.org

© 2013 Wiley-VCH Verlag GmbH & Co. KGaA, Weinheim

Angew. Chem. Int. Ed. **2013**, 52, 8880–8896

higher clearing temperatures often also lead to higher viscosities. New compounds that break this correlation in an advantageous way are of highest interest to the materials developers. A new single compound, however, is only part of the solution, since a suitable set of properties cannot be achieved with a single material. Instead, a mixture of up to 30 compounds has to be optimized to fulfill the LCD manufactures' request.

8. Polymer-Stabilized LC Modes

New display applications that combine the established nematic or chiral nematic liquid crystals with polymers have recently been growing in importance. Polymer-dispersed liquid crystals (PDLCs) with a polymer concentration of about 20 wt% are often discussed for projection displays or nondisplay LC applications such as switchable ("smart") windows.[57] Rapid development is also occurring in the lower polymer concentration range because of the ability to form polymer networks that stabilize liquid-crystal textures and improve their electrooptical performance. Polymer stabilization by surface modification can, in principle, be applied to different LC modes, but it is only used practically in multi-domain vertical alignment LC modes. A potential new application, where the polymer stabilization of the bulk is essential to widen the temperature range, makes use of polymer-stabilized blue phases (PS-BPs).[58]

8.1. Polymer-Stabilized Vertical Alignment (PS-VA)

An advanced technology that solves the intrinsic problems of the conventional VA modes (such as relatively low transmittance and strong gray scale dependency of the switching-on times at high operating voltages) is the polymer-sustained alignment (PSA) or polymer-stabilized VA (PS-VA) technology.[59] Today, PS-VA is the dominant commercial VA technology for TV displays.

Conventional VA modes have to overcome the problem that standard homeotropic alignment materials do not generate a uniform tilt angle. Special techniques such as the introduction of so-called protrusions in MVA[9] or electric fringe fields, as in PVA technology,[11] have to be applied to obtain defined switching without defect formation. In PS-VA, the polymerization creates a polymer network at the substrate surface that generates a tilt angle. UV-curable monomers, so-called reactive mesogens (RMs), are added to the VA-LC mixture in concentrations of < 1 wt%[60] and filled into the display. A voltage larger than the threshold voltage is subsequently applied so that the RM monomer as well as the LC reorients with a slight tilt angle from a vertical alignment. After irradiation with UV light, the monomers are polymerized and a "pretilt" angle is formed which remains even after removing the voltage. The rate at which the polymer layer is formed and the resulting pretilt angle depend on the structure of the UV-curable RM and the process conditions. RMs for PS-VA must be sufficiently soluble in the LC host so that, for example, the low-temperature stability of the

the system is not compromised. In addition, the monomer must not react in an uncontrolled manner to heat and UV load during panel fabrication. RMs showing good compatibility with the LC host are the compounds RM-257 (**108**) and RM-84 (**109**; Scheme 16).
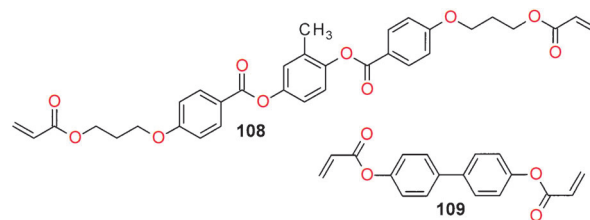
Scheme 16. Examples of RMs for PS-VA applications.

The development of effective RMs for the fast generation of a tilt angle that results in faster tact times in the production lines as well as specific PS-VA mixtures with high reliability are major tasks for materials development. In addition, the PS-VA process parameters, for example, doses of UV light or addressing voltages during the PS-VA process, are very important for the final pretilt angle in the display. In other words, the development focus is very much shifted from the liquid crystal to the reactive monomer and the PS-VA process optimization.

8.2. Polymer-Stabilized Blue-Phase Technology (PS-BP)

Blue phases (BPs) have attracted much interest because of their unique characteristics: According to the current understanding, chiral nematic liquid crystals form helical "double-twist cylinders" which in turn pack in an arrangement with cubic symmetry and with a lattice constant on the order of the wavelength of visible light.[46] Bragg reflection then gives rise to the eponymous blue color. However, mainly because of their narrow temperature range of only a few Kelvin or less, these fascinating mesophases were not considered suitable for display applications. In PS-BP, on the other hand, a true volume polymerization is realized, which stabilizes and extends the blue-phase temperature range to over 60 K.[58]

The polymer-stabilized blue phase as a switching medium in an LCD offers new possibilities for the next generation display technology because of intrinsic advantages such as ultrafast response times, no need for alignment layers, an optically isotropic dark state, high contrast with almost no viewing angle dependency, and cell-gap independency.

The underlying materials technology is based on specifically developed LC mixtures ("hosts") in combination with reactive mesogens, where the concentration of the RM is typically around 10 wt%. The most important parameters for PS-BP materials are an optimized host system and efficient polymer stabilization. The operating voltage typically increases with increasing RM concentration. The optimum is reached when the stabilization of the blue phase together with the lowest possible operating voltage is achieved. For

this, a very good compatibility of the blue-phase host with the RM system—typically consisting of one monofunctional and one difunctional RM—has to be ensured. Both the operating voltage and the phase stability can be improved significantly by using specifically designed RM systems.

To render an RM suitable for PS-BP, no premature polymerization must occur under normal storage conditions or during panel fabrication and processing. The compatibility with the host is important, that is, the monomer must be highly soluble and chemically stable in the host. The polymerization has to be controllable and reasonably fast for optimized production tact times. A complete polymerization is essential, that is, no residual RMs should be present in the host after the polymerization step so as to avoid subsequent uncontrolled reactions in the panel. Finally, it is crucial to find the lowest RM concentration that gives the optimum stabilization, as any excess polymer adversely affects the operating voltage.[61]

It is also necessary to maintain the blue-phase structure during polymerization of the RM to meet the requirements for a practicable stabilization process at a defined temperature. The typical BPs with reflection wavelengths in the visible light spectrum and bluish or greenish appearance are not useful for display applications, because of the non-accessible black off-state. As a consequence of the optical isotropic behavior of the blue phase, a good black state of the display can be realized by tuning the amount of chiral dopant in the LC mixture and thus shifting the reflection wavelength of the BP into the UV region. These so-called "invisible" BPs can then be used for display applications without color artifacts.

As a result of the intrinsic optical isotropy (cubic symmetry!), it is also necessary to adjust the birefringence so as to achieve the required retardation in the on-state. This can be done by using an electric field parallel to the glass substrates of the display together with a highly polar LC mixture ($\Delta\varepsilon > 100$ in the nematic phase). Nevertheless, high operating voltages are still major challenges for these displays.

All these requirements can be influenced by the development of mixtures with an appropriate combination of suitable RMs, chiral dopant, and LC components.

9. Conclusions and Outlook

Liquid-crystal material development in the two decades since 1990 has led to the successful commercialization of flat-screen computer monitors and large television sets. Today, these are established markets that already show signs of some saturation. On the other hand, we have recently witnessed a paradigm shift in personal computing and web access. Desktop computers appear old-fashioned to many consumers, and even laptop and ultrabook type computers are losing attractiveness in favor of portable smart phones and tablet PCs. Web access through these devices (the "TV in your pocket") already has a significant share, and it will grow quickly. LC materials have also changed in the course of this development. The breakthrough in mobile devices was

achieved by introducing easy to use touch screens that led to a boom in IPS and FFS LCD technologies that support the touch-panel functionality. These shifts in product popularity had to be taken into account in the development of liquid-crystal materials. Polymer-stabilized VA is increasingly replacing traditional VA, and the research focus at present is not only on new mesogenic structures, but also on suitable monomers for polymer formation in the display panel. For the liquid crystal itself, reliability, low viscosity, and last but not least cost-efficient chemical production will continue to be major driving forces for material development in years to come. New display modes such as a polymer-stabilized blue-phase mode could lead to extremely fast switching displays that are relatively cheap to produce, but need a complex materials system made up of monomeric liquid crystals, polymer networks, and chiral dopants. It is the combination of all these crucial components that will determine the quality of the final display—a new challenge for liquid crystal materials research for many years to come.

[1] M. Schadt, W. Helfrich, *Appl. Phys. Lett.* **1971**, *18*, 127–128.

[2] T. J. Scheffer, J. Nehring, *Appl. Phys. Lett.* **1984**, *45*, 1021–1023.

[3] K. Tarumi, M. Bremer, T. Geelhaar, *Annu. Rev. Mater. Sci.* **1997**, *27*, 423–441.

[4] a) M. Hird, *Chem. Soc. Rev.* **2007**, *36*, 2070–2095; b) P. Kirsch, M. Bremer, *Angew. Chem.* **2000**, *112*, 4384–4405; c) D. Pauluth, K. Tarumi, *J. Mater. Chem.* **2004**, *14*, 1219–1227.

[5] P. Kirsch, V. Reiffenrath, M. Bremer, *Synlett* **1999**, 389–396.

[6] a) R. Kiefer, B. Weber, F. Winscheid, G. Baur, *Proc. 12th Int. Displ. Res. Conf.* **1992**, 547–550 (Hiroshima, Japan) (Society of Information Display and the Institute of Television Engineers of Japan); b) M. Oh-e, K. Kondo, *Liq. Cryst.* **1997**, *22*, 379–390, and references therein.

[7] a) S. H. Lee, S. L. Lee, H. Y. Kim, *Appl. Phys. Lett.* **1998**, *73*, 2881–2883; b) I. H. Yu, I. S. Song, J. Y. Lee, S. H. Lee, *J. Phys. D* **2006**, *39*, 2367–2372; c) Y. J. Lim, M.-H. Lee, G.-D. Lee, W.-G. Jang, S. H. Lee, *J. Phys. D* **2007**, *40*, 2759–2764.

[8] M. Schiekel, K. Fahrenschon, *Appl. Phys. Lett.* **1971**, *19*, 391–393.

[9] A. Takeda, S. Kataoka, T. Sasaki, H. Chida, H. Tsuda, K. Ohmuro, Y. Koike, T. Sasabayashi, K. Okamoto, *SID Digest* **1998**, *29*, 1077–1080.

[10] Y. Ishii, S. Mizushima, M. Hijikigawa, *SID Digest* **2001**, *32*, 1090–1093.

[11] K. H. Kim, K. Lee, S. B. Park, J. K. Song, S. Kim, J. H. Souk, *Asia Display* **1998**, 383–386.

[12] a) E. Bartmann, K. Tarumi, (Merck KGaA), Patent DE 19531165, **1995** [*Chem. Abstr.* **1996**, *124*, 328585]; b) T. Ando, K. Shibata, S. Matsui, K. Miyazawa, H. Takeuchi, Y. Hisatsune, F. Takeshita, E. Nakagawa, K. Kobayashi, Y. Tomi, (Chisso Corp.), Patent EP 0844229, **1998** [*Chem. Abstr.* **1998**, *129*, 60620].

[13] P. Kirsch, M. Bremer, F. Huber, H. Lannert, A. Ruhl, M. Lieb, T. Wallmichrath, *J. Am. Chem. Soc.* **2001**, *123*, 5414–5417.

[14] a) A. Haas, M. Spitzer, M. Lieb, *Chem. Ber.* **1988**, *121*, 1329–1340; b) E. Bartmann, *Adv. Mater.* **1996**, *8*, 570–573.

[15] a) B. S. Pederson, S. Scheibye, K. Clausen, S. O. Lawesson, *Bull. Soc. Chim. Belg.* **1978**, *87*, 293–297; b) T. Kondo, K. Kobayashi, S. Matsui, H. Takeuchi, (Chisso Corp.), Patent DE 19946228, **1998** [*Chem. Abstr.* **2000**, *132*, 258446]; c) P. Kirsch, A. Ruhl, A. Hahn, T. Wallmichrath, unpublished results, **1999**.

[16] P. Kirsch, M. Bremer, A. Taugerbeck, T. Wallmichrath, *Angew. Chem.* **2001**, *113*, 1528–1532; *Angew. Chem. Int. Ed.* **2001**, *40*, 1480–1484.

[17] Preparation analogous to the methods described in: D. J. Ager, *Org. React.* **1990**, *38*, 1–223.

[18] The phase-transition temperatures are given in °C, the γ_1 values in mPa s. C = crystalline, S_x = smectic X, N = nematic, I = isotropic. T_{NI}, T_{NI} = nematic to isotropic transition temperature. Δn, and γ_1 were determined by linear extrapolation from a 10 wt% solution in the commercially available Merck mixture ZLI-4792 (T_{NI} = 92.8°C, $\Delta\varepsilon$ = 5.3, Δn = 0.0964). The extrapolated values are corrected empirically for differences in the order parameter. For dielectrically negative materials, $\Delta\varepsilon$ was extrapolated from ZLI-2857 (T_{NI} = 82.3°C, $\Delta\varepsilon$ = −1.4, Δn = 0.0776). For the pure substances, the mesophases were identified by optical microscopy, and the phase-transition temperatures by differential scanning calorimetry (DSC).

[19] P. Kirsch, M. Bremer, *ChemPhysChem* **2010**, *11*, 357–360.

[20] a) J. D. Roberts, G. S. Hammond, D. J. Cram, *Annu. Rev. Phys. Chem.* **1957**, *8*, 299–330; b) D. Holtz, *Prog. Phys. Org. Chem.* **1971**, *8*, 1–74; c) L. Radom, W. J. Hehre, J. A. Pople, *J. Am. Chem. Soc.* **1972**, *94*, 2371–2381; d) R. Hoffmann, L. Radom, J. A. Pople, P. von R. Schleyer, W. J. Hehre, L. Salem, *J. Am. Chem. Soc.* **1972**, *94*, 6221–6223.

[21] P. Kirsch, W. Binder, A. Hahn, K. Jährling, M. Lenges, L. Lietzau, D. Maillard, V. Meyer, E. Poetsch, A. Ruhl, G. Unger, R. Fröhlich, *Eur. J. Org. Chem.* **2008**, 3479–3487.

[22] H. Gilman, R. L. Bebb, *J. Am. Chem. Soc.* **1939**, *61*, 109–112.

[23] G. Wittig, G. Fuhrman, *Chem. Ber.* **1940**, *73*, 1197–1218.

[24] V. Snieckus, *Chem. Rev.* **1990**, *90*, 879–933.

[25] V. Reiffenrath, J. Krause, H. J. Plach, G. Weber, *Liq. Cryst.* **1989**, *5*, 159–170.

[26] V. Reiffenrath, M. Bremer, *Angew. Chem.* **1994**, *106*, 1435–1438.

[27] S. Achelle, N. Plé, A. Turck, *RSC Adv.* **2011**, *1*, 364–388.

[28] Y. Gotoh, *Mol. Cryst. Liq. Cryst.* **2011**, *542*, 16–27.

[29] a) T. Kusumoto, Y. Nagashima, S. Takehara, T. Matsumoto, (Chisso Corp.), Patent WO 2004029015, **2003** [*Chem. Abstr.* **2003**, *140*, 312432]; b) Y. Nagashima, T. Kusumoto, *Fain Kemikaru* **2008**, *37*, 17–22.

[30] K. Tarumi, M. Bremer, V. Reiffenrath, Patent DE 19900517, **1999** [*Chem. Abstr.* **1999**, *131*, 123055].

[31] M. Bremer, L. Lietzau, *New J. Chem.* **2005**, *29*, 72–74.

[32] V. P. Reddy, M. Perambuduru, R. Alleti, *Adv. Org. Synth.* **2006**, *2*, 327–351.

[33] S. C. Sondej, J. A. Katzenellenbogen, *J. Org. Chem.* **1986**, *51*, 3508–3513.

[34] M. Bremer, V. Meyer, unpublished results.

[35] a) V. Vill, H.-W. Tunger, K. Diekmann, *Tetrahedron: Asymmetry* **1994**, *5*, 2443–2446; b) V. Vill, H.-W. Tunger, *J. Chem. Soc. Chem. Commun.* **1995**, *10*, 1047–1048; c) V. Vill, H.-W. Tunger, *Liebigs Ann.* **1995**, *6*, 1055–1060; d) V. Vill, H.-W. Tunger, M. von Minden, *J. Mater. Chem.* **1996**, *6*, 739–746; e) B. Bertini, C. Moineau, D. Sinou, G. Gesekus, V. Vill, *Eur. J. Org. Chem.* **2001**, 375–382; f) B. Bertini, M. Perrin, D. Sinou, A. Thozet, V. Vill, *J. Carbohydr. Chem.* **2003**, *22*, 685–704.

[36] P. Kirsch, E. Poetsch, *Adv. Mater.* **1998**, *10*, 602–606.

[37] "Synthesis and Application of Chiral Liquid Crystals": D. Pauluth, A. E. F. Wächtler, *Chirality in Industry II* (Eds.: A. N. Collins, G. N. Sheldrake, J. Crosby), Wiley, New York, **1997**, pp. 263–286.

[38] J. Parsch, J. W. Engels, *Helv. Chim. Acta* **2000**, *83*, 1791–1808.

[39] a) S. Chang, R. H. Grubbs, *J. Org. Chem.* **1998**, *63*, 864–866; b) J. D. Rainier, S. P. Allwein, *J. Org. Chem.* **1998**, *63*, 5310–5311; c) J. M. Percy, S. Pintat, *Chem. Commun.* **2000**, 607–608; d) M. de Rosa, A. Solladie-Cavallo, A. Scettri, *Tetrahedron Lett.* **2000**, *41*, 1593–1596; e) M. A. Walters, F. La, P. Deshmukh, D. O. Omecinsky, *J. Comb. Chem.* **2002**, *4*, 125–130; f) X. Teng,

D. R. Cefalo, R. R. Schrock, A. H. Hoveyda, *J. Am. Chem. Soc.* **2002**, *124*, 10779–10784; g) L. C. Usher, M. Estrella-Jimenez, I. Ghiviriga, D. L. Wright, *Angew. Chem.* **2002**, *114*, 4742–4744; *Angew. Chem. Int. Ed.* **2002**, *41*, 4560–4562.

[40] a) R. J. Ferrier, W. G. Overend, M. A. E. Ryan, *J. Chem. Soc.* **1962**, 3667–3670; b) G. Grynkiewicz, A. Zamojski, *Z. Naturforsch. B* **1980**, *35*, 1024–1027.

[41] a) P. Kirsch, D. Maillard, *Eur. J. Org. Chem.* **2006**, 3326–3331; b) Ref. [21].

[42] "Development History of Liquid Crystal Displays": M. Bremer, M. Klasen-Memmer, K. Tarumi, *Progess in Liquid Crystal (LC) Science and Technology* (Eds.: H. S. Kwok, S. Naemura, H. L. Ong), World Scientific, Singapore, **2013**, pp. 97–111.

[43] a) A. J. Kirby, *The Anomeric Effect and Related Stereoelectronic Effects at Oxygen*, Springer, Berlin, **1983**; b) D. O'Hagan, H. S. Rzepa, *Chem. Commun.* **1997**, 645–652.

[44] Gaussian 09 (Revision B.01), M. J. Frisch, G. W. Trucks, H. B. Schlegel, G. E. Scuseria, M. A. Robb, J. R. Cheeseman, G. Scalmani, V. Barone, B. Mennucci, G. A. Petersson, H. Nakatsuji, M. Caricato, X. Li, H. P. Hratchian, A. F. Izmaylov, J. Bloino, G. Zheng, J. L. Sonnenberg, M. Hada, M. Ehara, K. Toyota, R. Fukuda, J. Hasegawa, M. Ishida, T. Nakajima, Y. Honda, O. Kitao, H. Nakai, T. Vreven, J. A. Montgomery, Jr., J. E. Peralta, F. Ogliaro, M. Bearpark, J. J. Heyd, E. Brothers, K. N. Kudin, V. N. Staroverov, T. Keith, R. Kobayashi, J. Normand, K. Raghavachari, A. Rendell, J. C. Burant, S. S. Iyengar, J. Tomasi, M. Cossi, N. Rega, J. M. Millam, M. Klene, J. E. Knox, J. B. Cross, V. Bakken, C. Adamo, J. Jaramillo, R. Gomperts, R. E. Stratmann, O. Yazyev, A. J. Austin, R. Cammi, C. Pomelli, J. W. Ochterski, R. L. Martin, K. Morokuma, V. G. Zakrzewski, G. A. Voth, P. Salvador, J. J. Dannenberg, S. Dapprich, A. D. Daniels, O. Farkas, J. B. Foresman, J. V. Ortiz, J. Cioslowski, D. J. Fox, Gaussian, Inc., Wallingford CT, **2010**.

[45] A. Taugerbeck, P. Kirsch, D. Pauluth, J. Krause, J. Suermann, M. Heckmeier, (Merck KGaA), Patent WO 02/94805, **2001** [*Chem. Abstr.* **2003**, *138*, 9737].

[46] a) A. Saupe, *Mol. Cryst. Liq. Cryst.* **1969**, *7*, 59–74; b) H. Stegemeyer, T. Blümel, K. Hiltrop, H. Onusseit, F. Porsch, *Liq. Cryst.* **1986**, *1*, 3–28.

[47] a) W. A. Sheppard, *J. Am. Chem. Soc.* **1960**, *82*, 4751–4752; b) W. A. Sheppard, *J. Am. Chem. Soc.* **1962**, *84*, 3064–3071; c) W. A. Sheppard, *J. Am. Chem. Soc.* **1962**, *84*, 3072–3076; d) H. L. Roberts, *J. Chem. Soc.* **1962**, 3183–3185.

[48] a) R. D. Chambers, M. P. Greenhall, J. Hutchinson, J. S. Moilliet, J. Thomson, *Abstract of Papers*, in: *Proc. 211th Natl. Meeting Am. Chem. Soc.*, New Orleans, LA, March 24–26, **1996**, American Chemical Society, Washington, DC, **1996**, FLUO 11; b) M. P. Greenhall, *15th International Symposium on Fluorine Chemistry*, Vancouver, Canada, Aug. 2–7, **1997**, presentation FRx C-2; c) R. D. Bowden, M. P. Greenhall, J. S. Moillet, J. Thomson, (F2 Chemicals), Patent WO 97/05106, **1997** [*Chem. Abstr.* **1997**, *126*, 199340]; d) R. D. Bowden, M. P. Greenhall, J. S. Moillet, J. Thomson, (F2 Chemicals), Patent US 5741935, **1997** [*Chem. Abstr.* **1997**, *126*, 199340.

[49] a) T. Umemoto, (IM&T Research, Inc.), Patent WO 2010/014665, **2008**; b) T. Umemoto, L. M. Garrick, N. Saito, *Beilstein J. Org. Chem.* **2012**, *8*, 461–471.

[50] a) J. Wessel, H. Hartl, K. Seppelt, *Chem. Ber.* **1986**, *119*, 453–463; b) T. Henkel, A. Klauck, K. Seppelt, *J. Organomet. Chem.* **1995**, *501*, 1–6; c) S. Aït-Mohand, W. R. Dolbier, Jr., *Org. Lett.* **2002**, *4*, 3013–3015; d) R. W. Winter, G. L. Gard, *J. Fluorine Chem.* **2004**, *125*, 549–552; e) T. A. Sergeeva, W. R. Dolbier, *Org. Lett.* **2004**, *6*, 2417–2419; f) P. Kirsch, J. Binder, E. Lork, G.-V. Röschenthaler, *J. Fluorine Chem.* **2006**, *127*, 610–619.

[51] a) P. Kirsch, M. Bremer, M. Heckmeier, K. Tarumi, *Angew. Chem.* **1999**, *111*, 2174–2178; *Angew. Chem. Int. Ed.* **1999**, *38*, 1989–1992; b) R. D. Bowden, P. J. Comina, M. P. Greenhall,

B. M. Kariuki, A. Loveday, D. Philp, *Tetrahedron* **2000**, *56*, 3399–3408.

[52] P. Kirsch, A. Hahn, *Eur. J. Org. Chem.* **2005**, 3095–3100.

[53] P. Kirsch, A. Hahn, *Eur. J. Org. Chem.* **2006**, 1125–1131.

[54] In analogy to: P. Kirsch, M. Bremer, A. Kirsch, J. Osterodt, *J. Am. Chem. Soc.* **1999**, *121*, 11277–11280.

[55] a) M. Bremer, K. Tarumi, *Adv. Mater.* **1993**, *5*, 842–848; b) M. Klasen, M. Bremer, A. Götz, A. Manabe, S. Naemura, K. Tarumi, *Jpn. J. Appl. Phys.* **1998**, *37*, L945–L948.

[56] a) A. Sasaki, T. Uchida, S. Miyagami, *Japan Display* **1986**, 62; b) M. Schadt, *Displays* **1992**, *13*, 11–34.

[57] C. M. Lampert, *Sol. Energy Mater. Sol. Cells* **2003**, *76*, 489–499.

[58] H. Kikuchi, M. Yokota, Y. Hisakado, H. Yang, T. Kajiyama, *Nat. Mater.* **2002**, *1*, 64–68.

[59] a) K. Hanaoka, Y. Nakanishi, Y. Inoue, S. Tanuma, Y. Koike, K. Okamoto, *SID Digest* **2004**, *35*, 1200–1203; b) S. G. Kim, S. M. Kim, S. K. Youn, H. K. Lee, S. H. Lee, G.-D. Lee, J. J. Lyu, K. H. Kim, *Appl. Phys. Lett.* **2007**, *90*, 261910; c) T. S. Chen, C. W. Huang, C. C. Hsieh, B. H. Huang, J. H. Jian, T. W. Chan, C. H. Tsao, C. W. Chen, C. Y. Chen, C. H. Chiu, C. H. Pai, J. H. Jaw, H. C. Lin, C. Y. Chiu, J. J. Su, S. Norio, T. J. Chang, W. L. Liau, A. Lien, *SID Digest* **2009**, *40*, 776–779.

[60] a) A. Götz, M. Klasen-Memmer, M. Bremer, A. Taugerbeck, K. Tarumi, D. Pauluth, *Proc. IDW 08* **2008**, 1527–1530; b) A. Götz, A. Taugerbeck, G. Bernatz, K. Tarumi, *SID Digest* **2010**, 718–720.

[61] M. Wittek, N. Tanaka, D. Wilkes, M. Bremer, D. Pauluth, J. Canisius, A. Yeh, R. Yan, K. Skjonnemand, M. Klasen-Memmer, *SID Digest* **2012**, *43*, 25–28.